# Ground Response to Tunnel Re-profiling Under Heavily Squeezing Conditions



**Originally published in:**
Rock Mechanics and Rock Engineering 49(7), https://doi.org/10.1007/s00603-016-0931-2

Rock Mech Rock Eng (2016) 49:2753–2762
DOI 10.1007/s00603-016-0931-2

ORIGINAL PAPER

# Ground Response to Tunnel Re-profiling Under Heavily Squeezing Conditions

**Apostolos Vrakas**[1] · **Georgios Anagnostou**[1]

Received: 8 September 2015 / Accepted: 9 February 2016 / Published online: 27 February 2016


**Abstract** This paper presents a finite strain theoretical analysis of the ground response around highly deformed circular tunnel cross sections that are subjected to (repeated) re-profiling in order to re-establish the desired clearance. Plane strain axially symmetric conditions are considered, with linearly elastic, perfectly or brittle plastic rock behaviour according to the non-associated Mohr–Coulomb model. On the basis of this theoretical analysis, some practical questions are addressed with respect to the ground response curve, the maximum rock pressure (as carried by a practically rigid new temporary support) and the maximum wall convergence (as expected in the presence of a light new support) after re-profiling. Finally, the paper revisits the question of the effectiveness of a pilot tunnel with respect to the ground response during enlargement of the tunnel cross section.

**Keywords** Large deformations · Re-mining · Rock pressure · Squeezing · Tunnel convergence

## List of Symbols

| | |
|---|---|
| $a_0$, $a$ | Initial and current tunnel radius |
| $c$, $c_p$, $c_r$ | Cohesion and corresponding peak and residual values |
| $E$ | Elastic (Young's) modulus |
| $G$ | Shear modulus |
| $i$ | Auxiliary variable |
| $m$ | Function of friction angle |
| $r_0$, $r$ | Initial and current radius of a material point |
| $u$ | Radial displacement of a material point |
| $u_*$ | Radial displacement of the point lying on the elasto-plastic boundary |
| $u_a$ | Radial displacement at the tunnel wall |
| $u_\rho$ | Radial displacement at the elasto-plastic boundary |
| $u_I$ | Initial excavation-induced tunnel convergence |
| $u_R$ | Re-profiling-induced tunnel convergence |
| $\varepsilon_1$, $\varepsilon_3$ | Major and minor principal strain |
| $\varepsilon_r$, $\varepsilon_t$ | Radial and tangential strain |
| $\kappa$ | Function of dilation angle |
| $\nu$ | Poisson's ratio |
| $\rho_0$, $\rho$ | Initial and current radius of the plastic zone |
| $\sigma$, $\bar{\sigma}$ | Normal stress and transformed normal stress |
| $\sigma_0$ | Isotropic in situ stress |
| $\sigma_1$, $\sigma_3$ | Major and minor principal Cauchy stress |
| $\sigma_a$ | Support pressure |
| $\sigma_D$, $\sigma_{D,p}$, $\sigma_{D,r}$ | Uniaxial compressive strength and corresponding peak and residual values |
| $\sigma_R$ | Rock pressure exerted upon a rigid new support after re-profiling |
| $\sigma_s$ | Initial support pressure upon unloading |
| $\sigma_r$, $\sigma_t$ | Radial and tangential Cauchy stress |
| $\sigma_\rho$ | Radial stress at the elasto-plastic boundary |
| $\varphi$ | Friction angle |
| $\psi$ | Dilation angle |

## Superscripts

| | |
|---|---|
| el | Elastic strain component |
| pl | Plastic strain component |
| $(n)$ | $n$th Excavation stage value |

✉ Apostolos Vrakas
apostolos.vrakas@igt.baug.ethz.ch

[1] ETH Zurich, Stefano-Franscini-Platz 5, 8093 Zurich, Switzerland

## 1 Introduction

The only possible way to construct a tunnel through heavily squeezing ground under high overburden consists in excavating a larger profile (hereafter referred to as 'over-excavation') and using temporary supports that can accommodate large deformations. Therefore, a main problem when tunnelling through squeezing rock is that of a major reduction in the cross section beyond the values planned. Experience has shown that the magnitude of the rock pressure or displacement is often underestimated, resulting in damage to the temporary support or a violation of the clearance profile. Re-excavation of the tunnel then becomes necessary. Re-profiling works are costly, time-consuming and, if the temporary support is overstressed, also demanding from the working safety viewpoint. Although a larger over-excavation might seem economically advantageous, this is not always true, since the rock quality may not be as poor as expected, in which case there will remain a space that has to be completely filled with concrete (Kovári 1998). Experience has also shown that the new temporary support systems installed after re-excavation of highly deformed tunnel zones are not as heavily loaded as the ones they replace (Kovári 1998). In fact, in the early history of tunnelling, the temporary support systems consisted of timber elements, which were crushed by the rock pressure from large deformations and had to be systematically replaced (Kovári and Staus 1996). Typical recent examples involving very large deformation problems that necessitate re-profiling operations include the multifunctional Faido station in the Gotthard base tunnel (Ehrbar 2008; Fig. 1a), the Saint Martin La Porte access adit in the Lyon–Turin base tunnel (Rettighieri et al. 2008; Bonini and Barla 2012; Fig. 1b) and the Yacambú–Quibor water tunnel in Venezuela (Hoek and Guevara 2009).

There is no analysis in the literature of the ground response to re-profiling following the occurrence of very large deformations, which actually constitutes an unloading problem from a partially plastified initial state. Here, a finite strain theoretical analysis of the problem is presented (Sect. 2), on the basis of which some questions of interest for engineering practice are answered: the relationship between rock pressure and deformation of the re-profiled opening (Sect. 3); the rock pressure developing upon a practically rigid new support (Sect. 4); the deformations that develop if a very light support is installed after re-profiling (Sect. 5); and the effectiveness of an advancing pilot tunnel with respect to rock pressure reduction (Sect. 6). Finite strain theory, in contrast to small strain theory, allows for a rigorous definition of stresses and strains around the opening, given that the tunnel boundary is adjusted accordingly after excavation of the deformed ground. It is also worth recalling, given that the paper deals with cases of very large deformations, that small strain theory is sufficient up to wall convergences of 10 %. At higher convergences, it leads to a remarkable overestimation of ground deformations, predicting radial displacements which can be even greater than the excavated tunnel radius (see Vrakas and Anagnostou 2015 for a meticulous analysis of this topic).


**Fig. 1** Examples of tunnels necessitating re-profiling: **a** multifunction Faido station, Gotthard base tunnel, Switzerland (Ehrbar 2008); **b** Saint Martin La Porte access adit, Lyon–Turin base tunnel (Rettighieri et al. 2008)

## 2 Theoretical Analysis

### 2.1 Outline

A circular tunnel cross section far behind the face is considered under plane strain, rotationally symmetric conditions, with the axes' origin placed at its centre. The ground extends to infinity and is taken to be homogeneous, isotropic and linearly elastic–plastic. Experimental observations show that, for many rocks, once the peak strength is

reached, it is gradually reduced towards the residual one. This behaviour is commonly modelled using a trilinear stress–strain relationship (i.e. a constant drop modulus), but consideration of the strain-softening part complicates the theoretical analysis of the ground response problem (Borsetto and Ribacchi 1979; Alonso et al. 2003), even in the case that elastic strains are neglected in the plastic zone (Panet 1976). The two borderline cases of strain-softening behaviour will thus be considered, i.e. perfectly plastic (negligible rate of strength drop) and brittle plastic (very high rate of strength drop). Time-dependent effects are neglected. Assuming Mohr–Coulomb failure criterion and taking stresses as positive for compression, the major principal stress $\sigma_1$ at failure is expressed with respect to the minor principal stress $\sigma_3$ as follows:

$$\sigma_1 = m\sigma_3 + \sigma_{D,\mathrm{p}}, \tag{1}$$

where $m$ is a function of the friction angle $\varphi$:

$$m = \frac{1+\sin\varphi}{1-\sin\varphi}, \tag{2}$$

and $\sigma_{D,\mathrm{p}}$ is the peak uniaxial compressive strength:

$$\sigma_{D,\mathrm{p}} = \frac{2c_\mathrm{p}\cos\varphi}{1-\sin\varphi}, \tag{3}$$

where $c_\mathrm{p}$ stands for the peak cohesion. Considering the same friction angle for the residual state (Panet 1993), the failure criterion becomes

$$\sigma_1 = m\sigma_3 + \sigma_{D,\mathrm{r}}, \tag{4}$$

where the residual uniaxial compressive strength $\sigma_{D,\mathrm{r}}$ is related to the residual cohesion $c_\mathrm{r}$ analogously to Eq. (3). In the special case of ductile rock behaviour (exhibited, e.g., by the kakirites encountered in the Gotthard base tunnel; Vogelhuber et al. 2004), $\sigma_{D,\mathrm{p}} = \sigma_{D,\mathrm{r}} = \sigma_D$.

Using the following transformation of normal stresses to simplify the mathematical operations:

$$\bar{\sigma} = \sigma + \frac{\sigma_{D,\mathrm{r}}}{m-1}, \tag{5}$$

the failure criterion at the residual state (Eq. 4) becomes

$$\bar{\sigma}_1 = m\bar{\sigma}_3. \tag{6}$$

A non-associated plastic flow rule is further considered, which fixes the ratio of the principal plastic strain rates:

$$\frac{\dot{\varepsilon}_3^{\mathrm{pl}}}{\dot{\varepsilon}_1^{\mathrm{pl}}} = -\kappa, \tag{7}$$

with the coefficient $\kappa$ being expressed as a function of the dilation angle $\psi$:

$$\kappa = \frac{1+\sin\psi}{1-\sin\psi}. \tag{8}$$

Figure 2 illustrates the problem schematically. The opening of the initial radius $a_0^{(1)}$ is initially unloaded from a uniform and isotropic initial stress state of magnitude $\sigma_0$ (Fig. 2a). The ground behaves elastically until the failure criterion (Eq. 1) is satisfied at the tunnel wall ($r = a$) and it experiences increasing irreversible strains at lower support pressures $\sigma_a$, forming an expanding plastic ring of outer radius $\rho$. At the end of the first excavation, the tunnel and the plastic radii read $a^{(1)}$ and $\rho^{(1)}$, respectively, and the (predefined) support pressure equals $\sigma_a^{(1)}$ (Fig. 2b). If $a^{(1)}$ is smaller than the desired clearance, re-profiling must be performed.

From a computational viewpoint, excavation of the already deformed ground can be modelled as a gradually decreasing support pressure acting on the new tunnel boundary, taking the initial stress field of the continuum equal to that corresponding to the end of the first excavation. Therefore, the deformed ground lying within the radius $a_0^{(2)}$ (where $a_0^{(2)} = a_0^{(1)} = a_0$; the special case where $a_0^{(2)} > a_0^{(1)}$ is related to the problem of driving a pilot tunnel first, and this will be examined in Sect. 6) is excavated and the opening is unloaded from a partially plastified state under the support pressure $\sigma_s^{(2)}$ (Fig. 2c). This pressure corresponds to the radial stress at distance $r = a_0^{(2)}$ at the end of the first excavation. A new tunnel convergence takes place and the plastic zone at the end of the second excavation stage extends to the radius $\rho^{(2)}$ (Fig. 2d). If the tunnel radius $a^{(2)}$ (under the given support pressure $\sigma_a^{(2)}$) still fails to maintain the desired clearance, excavation of the deformed ground is repeated. This process continues until the desired clearance is maintained.

Experience shows that a single stage of re-profiling will suffice, regardless of the magnitude of the rock deformations following the first excavation, i.e. the new temporary support system will maintain the desired clearance without presenting structural problems, even in cases where an almost total tunnel closure has occurred prior to re-profiling. However, for the sake of generality, the following analysis is based on the $n$th excavation stage, where the opening is unloaded from a partially plastified state with plastic radius $\rho^{(n-1)}$ and initial support pressure $\sigma_s^{(n)}$. The first excavation stage, where the initial stress state is uniform and isotropic, is derived as a special case.

Logarithmic strains are considered in the plastic zone, but second and higher order terms are neglected in the outer elastic zone on the reasonable assumption that any elastic strains are small. Moreover, the simplifying assumption is made that elastic strains in the plastic zone are negligible (Panet 1993; Kovári 1998). The error introduced by this assumption depends on the material

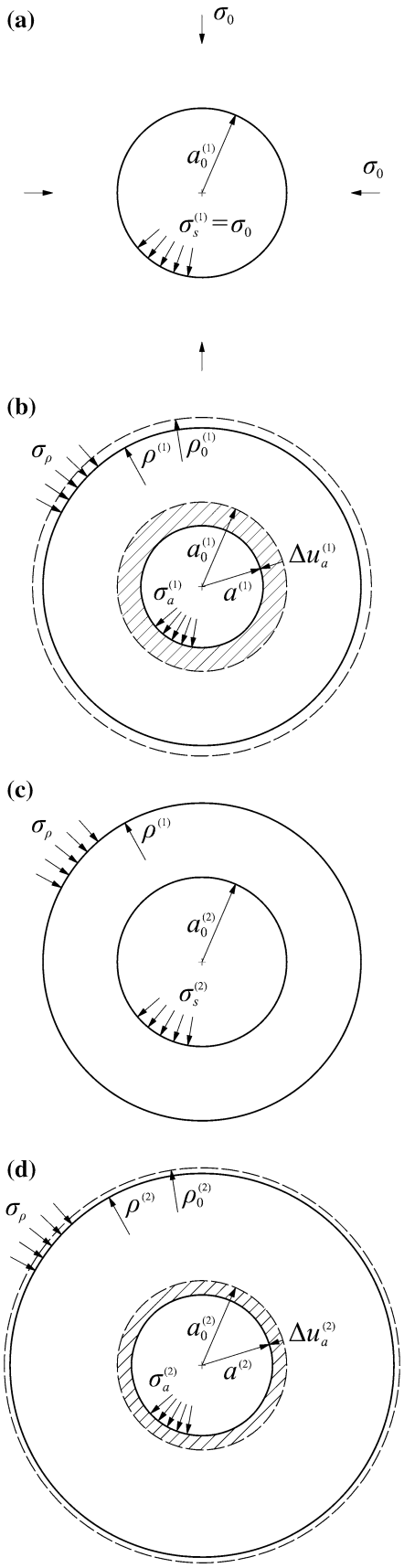


◀**Fig. 2** Setup of the tunnel re-profiling problem: **a** initial state; **b** state after excavation and support of pressure $\sigma_a^{(1)}$; **c** initial state for first re-profiling; **d** state after first re-profiling and support of pressure $\sigma_a^{(2)}$

constants and is generally small (up to 20 %) for deep tunnels under heavily squeezing conditions (Vrakas and Anagnostou 2014), becoming equal to zero in the special case of incompressible and non-dilatant ground behaviour (e.g. the behaviour underlying the instantaneous response of saturated ground to tunnel excavation).

### 2.2 Elastic Zone

The mean effective stress remains constant throughout elastic ground response. Considering further that the radial stress, $\sigma_\mathrm{r}$, is the minor principal stress while the tangential stress, $\sigma_\mathrm{t}$, is the major principal stress, the critical radial stress at yielding, $\sigma_\rho$, reads:

$$\sigma_\rho = \frac{2\sigma_0 - \sigma_{D,\mathrm{p}}}{m+1}. \tag{9}$$

Therefore, the elastic zone can be regarded as the ground around an opening of radius $\rho$ subject to the constant support pressure $\sigma_\rho$, in which the radial stress and displacement are given by the well-known Lamé's relationships:

$$\sigma_\mathrm{r} = \sigma_0 - (\sigma_0 - \sigma_\rho)\left(\frac{\rho}{r}\right)^2 \tag{10}$$

and

$$\frac{u}{r} = \frac{\sigma_0 - \sigma_\rho}{2G}\left(\frac{\rho}{r}\right)^2, \tag{11}$$

where displacements are taken as positive for contraction and the shear modulus $G$ is related to the elastic modulus $E$ and the Poisson's ratio $\nu$ by $G = E/[2(1+\nu)]$.

### 2.3 Stress Distribution in the Plastic Zone

In the following analysis, it is assumed that the out-of-plane stress continues to be the intermediate principal stress throughout unloading. (At low support pressures, the out-of-plane stress may become and remain equal to the tangential stress, i.e. to the major principal stress. The error from neglecting the out-of-plane plastic flow is, nevertheless, negligible; Vrakas and Anagnostou 2014).

The failure criterion (Eq. 6) is fulfilled throughout the plastic zone and, hence,

$$\bar{\sigma}_\mathrm{t} = m\bar{\sigma}_\mathrm{r}. \tag{12}$$

Substituting Eq. (12) into the stress equilibrium condition, namely

$$\frac{\mathrm{d}\bar{\sigma}_\mathrm{r}}{\mathrm{d}r}+\frac{\bar{\sigma}_\mathrm{r}-\bar{\sigma}_\mathrm{t}}{r}=0, \tag{13}$$

a differential equation is obtained with respect to the radial stress, whose integration over the interval $[a, r]$ yields

$$\bar{\sigma}_\mathrm{r}=\bar{\sigma}_a\left(\frac{r}{a}\right)^{m-1}. \tag{14}$$

Evaluating Eq. (14) at the elasto-plastic boundary at the end of the $n$th excavation stage gives the radius of the plastic zone (Fig. 2b, d):

$$\frac{\rho^{(n)}}{a^{(n)}}=\left(\frac{\bar{\sigma}_\rho}{\bar{\sigma}_a^{(n)}}\right)^{\frac{1}{m-1}}, \tag{15}$$

while evaluating Eq. (14) at the future excavation boundary (as long as $\rho^{(n)}\geq a_0^{(n+1)}$, Fig. 2c; otherwise Eq. 10 should be used) gives the initial support pressure for the next excavation stage:

$$\bar{\sigma}_s^{(n+1)}=\bar{\sigma}_a^{(n)}\left(\frac{a_0^{(n+1)}}{a^{(n)}}\right)^{m-1}. \tag{16}$$

(Note that at first unloading, $\sigma_s^{(1)}=\sigma_0$; Fig. 2a.) The support pressure after the $(n+1)$th excavation stage is reduced from $\sigma_s^{(n+1)}$ to the given value $\sigma_a^{(n+1)}$ (boundary condition).

### 2.4 Displacements in the Plastic Zone

A material point in the vicinity of the opening moves towards the tunnel wall during each excavation stage. Attention should be paid to the notation used here. The variable $r_0^{(n)}$ denotes the position of the material point in the initial state of the $n$th excavation stage and the variable $r^{(n)}$ denotes its position at the end. Therefore, $r_0^{(1)}$ corresponds to its position in the undisturbed state prevailing before tunnelling, whereas $r_0^{(n)}=r^{(n-1)}$ thereafter. The total displacement of the material point equals

$$u^{(n)}=r_0^{(1)}-r^{(n)} \tag{17}$$

and the displacement occurring during the $n$th excavation stage becomes

$$\Delta u^{(n)}=u^{(n)}-u^{(n-1)}=r_0^{(n)}-r^{(n)}. \tag{18}$$

By evaluating Eq. (18) at the tunnel wall and at the elasto-plastic boundary, we have

$$\Delta u_a^{(n)}=a_0^{(n)}-a^{(n)} \tag{19}$$

and

$$\Delta u_\rho^{(n)}=\rho_0^{(n)}-\rho^{(n)}, \tag{20}$$

respectively, where $\rho_0^{(n)}$ denotes the position of the material point lying now on the elasto-plastic interface in the initial state of the current excavation stage (note that $\rho_0^{(n)}\neq\rho^{(n-1)}$; Fig. 2). It should be emphasized that both the tunnel wall and the elasto-plastic boundary are not associated with the same material points in each excavation stage since the deformed ground within the radius $a_0^{(n)}$ is removed and the plastic zone $\rho^{(n-1)}$ extends outwards (Fig. 2).

The plastic flow rule implies that the ratio of the radial to the tangential plastic strain rate is constant (Eq. 7). Assuming that elastic strains are negligible relative to plastic strains inside the plastic zone, such that $\dot{\varepsilon}_\mathrm{r}=\dot{\varepsilon}_\mathrm{r}^\mathrm{el}+\dot{\varepsilon}_\mathrm{r}^\mathrm{pl}\cong\dot{\varepsilon}_\mathrm{r}^\mathrm{pl}$ and $\dot{\varepsilon}_\mathrm{t}=\dot{\varepsilon}_\mathrm{t}^\mathrm{el}+\dot{\varepsilon}_\mathrm{t}^\mathrm{pl}\cong\dot{\varepsilon}_\mathrm{t}^\mathrm{pl}$, and integrating Eq. (7) over the current excavation stage,

$$\Delta\varepsilon_\mathrm{r}^{(n)}+\kappa\,\Delta\varepsilon_\mathrm{t}^{(n)}=0, \tag{21}$$

where, in a similar way to Eq. (18), the radial and tangential strains developed during the $n$th excavation read

$$\Delta\varepsilon_\mathrm{r}^{(n)}=\varepsilon_\mathrm{r}^{(n)}-\varepsilon_\mathrm{r}^{(n-1)} \tag{22}$$

and

$$\Delta\varepsilon_\mathrm{t}^{(n)}=\varepsilon_\mathrm{t}^{(n)}-\varepsilon_\mathrm{t}^{(n-1)}. \tag{23}$$

According to the logarithmic definition of strains,

$$\Delta\varepsilon_\mathrm{r}^{(n)}=\ln\frac{\mathrm{d}r_0^{(n)}}{\mathrm{d}r^{(n)}} \tag{24}$$

and

$$\Delta\varepsilon_\mathrm{t}^{(n)}=\ln\frac{r_0^{(n)}}{r^{(n)}}. \tag{25}$$

Substituting Eqs. (24) and (25) into Eq. (21) and integrating the resulting differential equation over the region $\left[a^{(n)}, r^{(n)}\right]$, the following kinematic relationship is deduced:

$$\left(a_0^{(n)}\right)^{\kappa+1}-\left(a^{(n)}\right)^{\kappa+1}=\left(r_0^{(n)}\right)^{\kappa+1}-\left(r^{(n)}\right)^{\kappa+1}. \tag{26}$$

Including the material point at the plastic boundary, Eq. (26) becomes

$$\left(a_0^{(n)}\right)^{\kappa+1}-\left(a^{(n)}\right)^{\kappa+1}=\left(\rho_0^{(n)}\right)^{\kappa+1}-\left(\rho^{(n)}\right)^{\kappa+1}, \tag{27}$$

which for $\kappa=1$ expresses the condition of constant volume of the plastic zone. The material point lying now on the elasto-plastic boundary, denoted by '*', was previously in the elastic zone (Fig. 3). Therefore, as the deformations in the elastic zone are small, its total radial displacement at the end of the $(n-1)$th and at the end of the $n$th excavation step can be calculated using Eq. (11). Specifically,

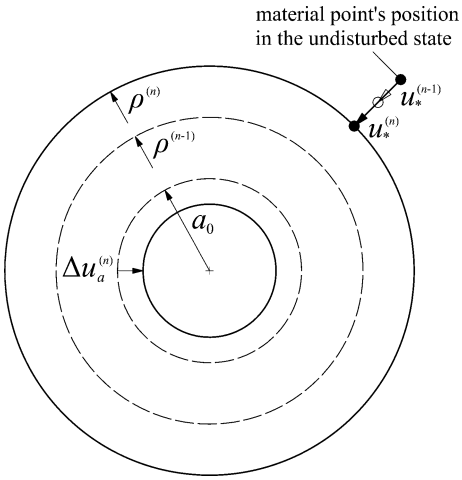


**Fig. 3** Schematic representation of the movement of the material point lying at the *n*th excavation stage on the elasto-plastic boundary

$$\frac{u_*^{(n-1)}}{\rho^{(n)}} = \frac{\bar{\sigma}_0 - \bar{\sigma}_\rho}{2G}\left(\frac{\rho^{(n-1)}}{\rho^{(n)}}\right)^2, \tag{28}$$

$$\frac{u_*^{(n)}}{\rho^{(n)}} = \frac{\bar{\sigma}_0 - \bar{\sigma}_\rho}{2G} \tag{29}$$

and $\Delta u_\rho^{(n)} = \rho_0^{(n)} - \rho^{(n)} = u_*^{(n)} - u_*^{(n-1)}$ (Fig. 3). Therefore,

$$\frac{\rho_0^{(n)}}{\rho^{(n)}} = 1 + \frac{\bar{\sigma}_0 - \bar{\sigma}_\rho}{2G}\left[1 - \left(\frac{\rho^{(n-1)}}{\rho^{(n)}}\right)^2\right]. \tag{30}$$

Substituting Eq. (30) into Eq. (27) and incorporating Eq. (15), the following non-linear algebraic equation with respect to the current tunnel radius $a^{(n)}$ is deduced:

$$\left(\frac{a_0^{(n)}}{a^{(n)}}\right)^{\kappa+1} = 1 + \left(\frac{\bar{\sigma}_\rho}{\bar{\sigma}_a^{(n)}}\right)^{\frac{\kappa+1}{m-1}} \left(\left\{1 + \frac{\bar{\sigma}_0 - \bar{\sigma}_\rho}{2G}\left[1 - \left(\frac{a^{(n-1)}}{a^{(n)}}\right)^2 \left(\frac{\bar{\sigma}_a^{(n)}}{\bar{\sigma}_a^{(n-1)}}\right)^{\frac{2}{m-1}}\right]\right\}^{\kappa+1} - 1\right). \tag{31}$$

A closed-form solution is derived for the first excavation (see also Yu and Rowe 1999):

$$\left(\frac{a_0^{(1)}}{a^{(1)}}\right)^{\kappa+1} = 1 + \left(\frac{\bar{\sigma}_\rho}{\bar{\sigma}_a^{(1)}}\right)^{\frac{\kappa+1}{m-1}} \left[\left(1 + \frac{\bar{\sigma}_0 - \bar{\sigma}_\rho}{2G}\right)^{\kappa+1} - 1\right]. \tag{32}$$

### 2.5 Summary of the Calculation Process

Equation (31) contains the tunnel radius at the end of the previous excavation. Therefore, the calculation of the ground response curve (GRC) for the *n*th excavation stage of a highly deformed circular tunnel cross section (i.e. the relationship between the support pressure $\sigma_a^{(n)}$ and the tunnel wall displacement $\Delta u_a^{(n)}$) requires the entire unloading history of the ground.

The calculation process is summarized in the following steps:

1. Initialize $i = 1$.
2. Compute the current tunnel radius $a^{(i)}$ after the *i*th excavation (Eq. 32 for $i = 1$; else Eq. 31), given the excavated tunnel radius $a_0^{(i)}$ and the final support pressure $\sigma_a^{(i)}$.
3. Set $i = i + 1$ and if $i < n$, go to (2).
4. Otherwise, compute the current tunnel radius $a^{(n)}$ (Eq. 31—and thus the tunnel convergence after Eq. 19), given the excavated tunnel radius $a_0^{(n)}$, by stepwise reduction of the support pressure $\sigma_a^{(n)}$ from $\sigma_s^{(n)}$ (Eq. 16) to zero.

Equation (31) can be solved by means of basic numerical methods (e.g. with the standard Newton–Raphson scheme).

## 3 Ground Response Curve After Re-profiling

Figure 4 concerns the computational example of a 1000 m deep tunnel crossing weak rock ($\sigma_D/\sigma_0 = 0.1$) and shows the GRCs for the initial excavation (dashed curve) and for the re-profiling (solid curves). The GRCs for re-profiling assume that the temporary support used in the initial excavation offers negligible resistance (curve A) or a light resistance of 0.5 MPa (curve B), respectively; points A and B on the dashed line show the state prevailing before re-profiling. Two main conclusions can be drawn from these results: (a) the rock pressure developing after re-profiling is moderate (up to 1.2 MPa in the present example) even if the new support is practically rigid; and, (b), in the presence of a very light new support, the re-profiling-induced convergences can still be very large (up to 45 % of the initial excavation-induced convergences here). These two aspects are analysed in detail in the next sections.

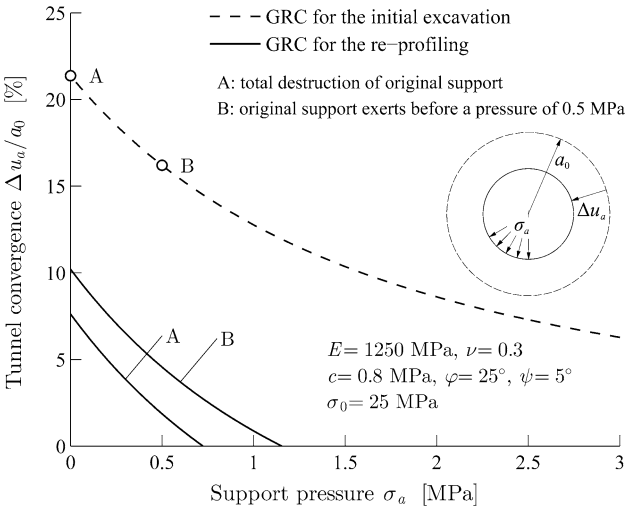


**Fig. 4** Ground response curves for the initial excavation and for the re-profiling

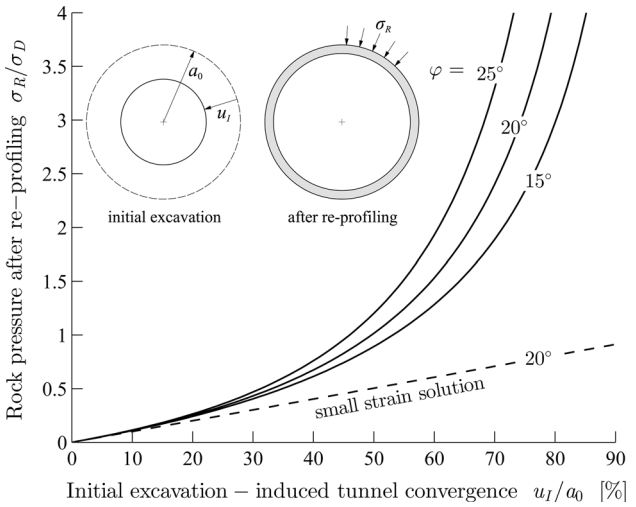


**Fig. 5** Maximum rock pressure developing upon a rigid support installed after re-profiling, based upon the wall convergence occurring after the initial excavation, assuming that the initial support provided negligible resistance

## 4 Upper Limit of Rock Pressure After Re-profiling (Exerted Upon a Practically Rigid New Temporary Support)

The rock pressure that would develop upon a practically rigid support after re-profiling of a highly deformed tunnel, as denoted by $\sigma_R$, can be explicitly calculated by means of Eq. (16). More specifically, assuming that the old temporary support offers negligible resistance ($\sigma_a^{(1)} = 0$), either because it is completely destroyed or because it is a yielding support of very low yielding pressure, Eq. (16) gives

$$\sigma_R = \frac{\sigma_D}{m-1}\left[\left(1-\frac{u_I}{a_0}\right)^{1-m}-1\right], \tag{33}$$

where $u_I$ denotes the tunnel convergence occurring in the initial excavation. In the case of brittle rock behaviour, $\sigma_D$ should be replaced by $\sigma_{D,\mathrm{r}}$. Note that the overburden, the elastic material constants and the dilatancy angle do not appear in this equation. Instead, Eq. (33) gives the rock pressure developing after re-profiling as a function of the convergence actually observed in the initial excavation, the friction angle and the uniaxial compressive strength of the rock mass (Fig. 5). It should be pointed out that Eq. (33) is derived solely from static considerations and is thus exact.

The generally applicable diagram in Fig. 5 allows a quick estimate to be made of the maximum rock pressure following re-profiling. It shows that for common cases, where the tunnel closure does not exceed half of the cross section, the support capacity required from the new temporary support system is relatively low, a fraction of the uniaxial compressive strength of the squeezing rock. This conclusion is in accordance with tunnelling experience, which shows that the linings installed after re-mining tunnel zones that have become deformed beyond acceptable limits do not present structural problems, even in cases of extreme squeezing conditions where the primary lining has practically collapsed and the tunnel cross section has closed almost completely (e.g. in the Yacambú-Quibor tunnel; Hoek and Guevara 2009).

Finally, the value of large strain theory in this context is worth demonstrating. By neglecting the geometric nonlinearity and thus positing equilibrium in the undeformed configuration, the radial stress around the opening reads (cf. Eq. 14)

$$\bar{\sigma}_{\mathrm{r}} = \bar{\sigma}_a\left(\frac{r}{a_0}\right)^{m-1}. \tag{34}$$

Therefore, an upper estimate of the radial stress at the future excavation boundary is given by the following relationship:

$$\sigma_R = \frac{\sigma_D}{m-1}\left[\left(1+\frac{u_I}{a_0}\right)^{m-1}-1\right]. \tag{35}$$

Figure 5 plots Eq. (35) for $\varphi = 20°$ (dashed curve) and shows that small strain theory grossly underestimates the rock pressure in the presence of extremely large deformations.

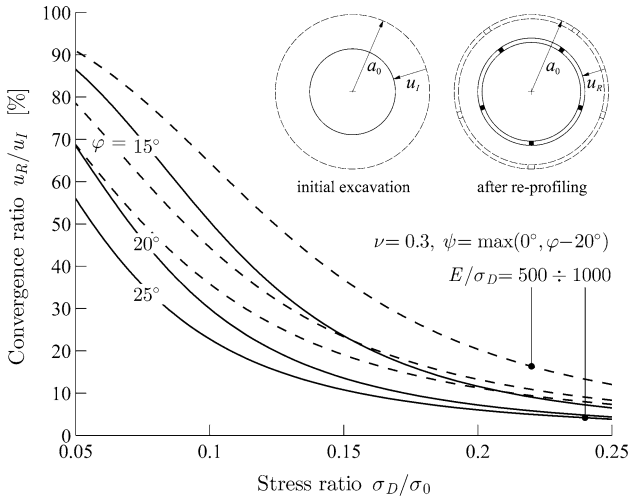


**Fig. 6** Ratio of re-profiling-induced to initial excavation-induced convergences, assuming that the new support provides negligible resistance for perfectly plastic rock behaviour

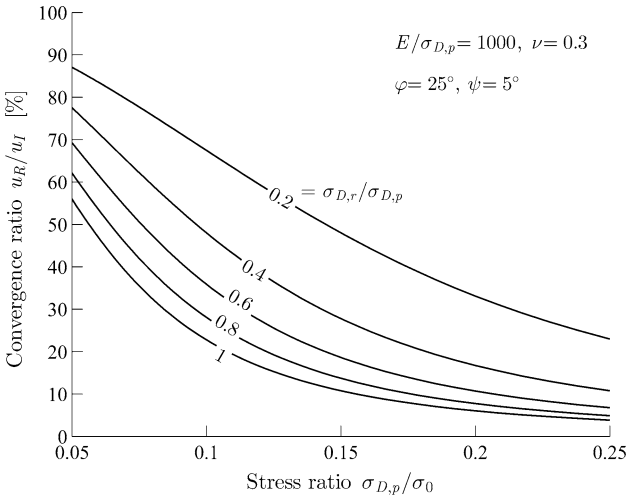


**Fig. 7** Ratio of re-profiling-induced to initial excavation-induced convergences, assuming that the new support provides negligible resistance for brittle plastic rock behaviour

## 5 Upper Limit of Tunnel Convergence After Re-profiling (in the Presence of a Very Light New Temporary Support)

The example of Sect. 3 indicated that, in the absence of a sufficient support resistance, the re-profiling-induced deformations may still be very large. Here, a more detailed analysis of this aspect is made. Figure 6 plots the ratio of the re-profiling-induced convergence, $u_R$, to the initial excavation-induced convergence, $u_I$, as a function of the stress ratio $\sigma_D/\sigma_0$ (assuming perfectly plastic behaviour). As can be seen, the lower the ratio of the unconfined rock strength to in situ stress, the higher is the ratio of tunnel convergences, reading up to 90 % in extreme cases and up to 35 % for common cases where $\sigma_D/\sigma_0 > 0.15$. This highlights the important role of the new temporary support, which—under heavily squeezing conditions—should have enough deformation capacity to accommodate the re-profiling-induced convergences. Figure 6 can be used (similarly to Fig. 5) considering what was actually observed in the initial excavation. More specifically, in the presence of a very light new support, the maximum convergence after re-excavation of the tunnel can be estimated on the basis of the observed deformation in the initial excavation and the convergence ratio provided by the present diagram.

Figure 7 plots the ratio of convergences $u_R/u_I$ for the case of brittle rock behaviour. As can be seen, the lower the residual compressive strength, the higher is the initial excavation-induced convergence and the corresponding percentage of the re-profiling-induced convergence.

It should be noted finally that large convergences would occur in the presence of a light support even after several re-profiling stages. Figure 8 shows the tunnel convergence during repeated re-profiling of a circular tunnel excavated through heavily squeezing rock. It is remarkable that the convergences do not vanish after a second re-profiling round for the case of perfectly plastic rock behaviour (provided that the support applied is always negligible; see lower curve), while high convergences continue to occur even after six excavation stages in the case of low residual compressive strength (see upper curve).

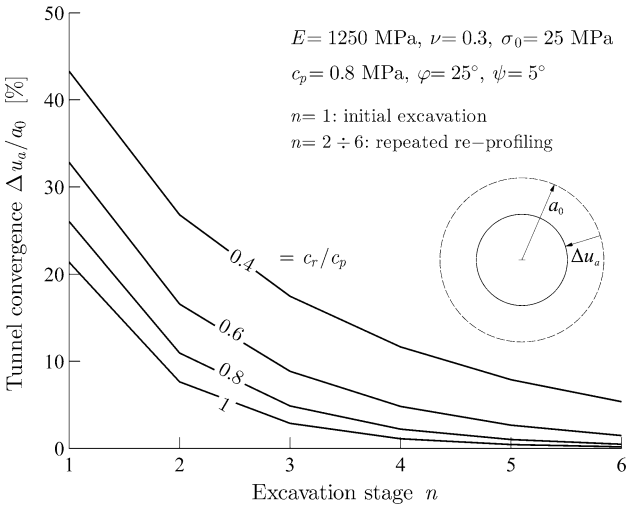


**Fig. 8** Convergence of an unsupported tunnel cross section during repeated re-profiling

## 6 Effectiveness of Driving a Pilot Tunnel First

Pilot tunnels cause initial deformations and stress relief in the surrounding rock mass. Kovári (1998) raised a question over the benefits of an advancing pilot tunnel in relation to

subsequent enlargement of the tunnel cross section and answered the question negatively, based on simplified purely geometric considerations. This section revisits this problem on the basis of the finite strain theoretical analysis presented above.

We consider again a 1000 m deep tunnel crossing weak rock (parameters as in Sect. 3). A pilot tunnel of radius equal to one-third of that of the full cross section is initially excavated (i.e. $a_0^{(2)} = 3a_0^{(1)} = a_0$ in the theoretical analysis) and enlarged later to the full cross section. To secure the maximum rock pressure relief prior to enlargement, we assume that the support of the pilot tunnel is very light (i.e. $\sigma_a^{(1)} = 0$ in the theoretical analysis). Figure 9 shows the GRC of the full cross section without (dashed curve) and with (solid curve) pre-construction of a pilot tunnel. The dashed curve also applies to the pilot tunnel, of course.

Although the excavation of the pilot tunnel causes a convergence of almost 20 %, the plastic zone extends only up to $1.2a_0$ (see inset in Fig. 9) and the convergence at the future excavation boundary amounts to just 2 %, which indicates that the stress relief around the future enlarged cross section cannot be high. Indeed, as can be seen in Fig. 9, the initial deformations caused by the pilot drift reduce the future maximum rock pressure (to 10 MPa, i.e. 40 % of the initial stress), but the maximum wall convergence remains approximately constant (20 vs. 21 %). These conclusions remain valid even when considering extreme squeezing conditions leading almost to a complete closure of the pilot tunnel (Fig. 10) or a smaller overburden (Fig. 11).

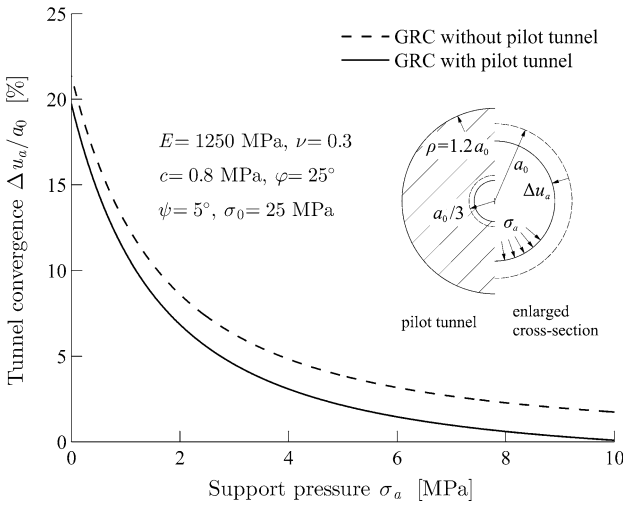


**Fig. 9** Ground response curves with and without first driving an unsupported pilot tunnel for the characteristic example of a 1000 m-deep tunnel through heavily squeezing ground (*inset* in scale)

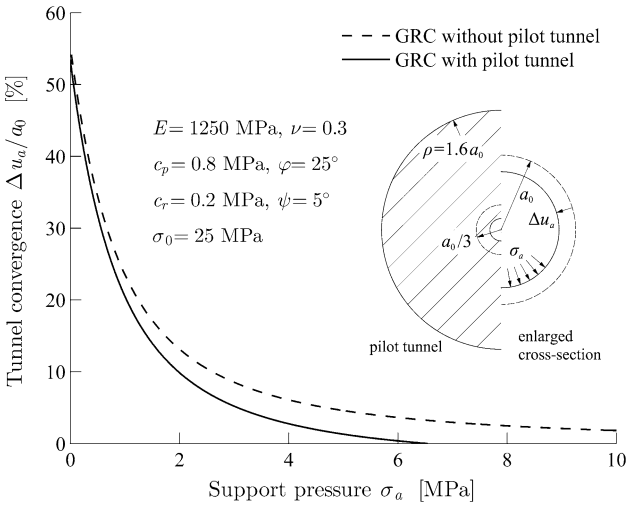


**Fig. 10** Ground response curves with and without first driving an unsupported pilot tunnel for the characteristic example of a 1000 m-deep tunnel through extreme squeezing conditions, leading almost to closure of the pilot tunnel (*inset* in scale)

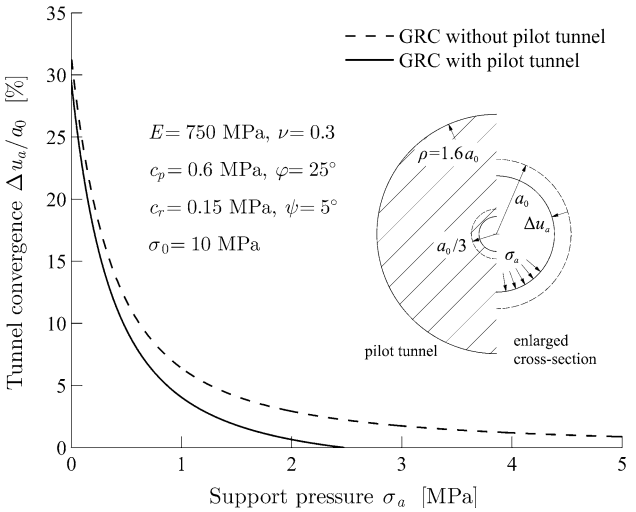


**Fig. 11** Ground response curves with and without first driving an unsupported pilot tunnel for the characteristic example of a 400 m-deep tunnel through heavily squeezing ground (*inset* in scale)

Therefore, according to the presented computational resuts, driving a pilot tunnel first just to de-stress the surrounding rock does not seem to offer a benefit over a solution based on over-excavation and use of yielding supports. The conclusion about the effectiveness of a pilot tunnel is in accordance with Kovári's (1998) standpoint that the construction of a pilot tunnel is not justified economically. It should be noted, however, that a pilot tunnel in water-bearing ground can provide pore pressure relief ahead of the excavation. Advance drainage is favourable with respect to the intensity of squeezing (Steiner 1996; Kovári 1998; Anagnostou 2009a, 2009b).

## 7 Closing Remarks

The paper presented a large strain elasto-plastic analysis of the ground response to tunnel re-profiling under heavily squeezing conditions, a problem involving cavity unloading from a partially plastified initial state. The calculation of the characteristic line of the rock requires the solution of a simple non-linear algebraic equation, which incorporates the wall convergence that took place in the previous excavation stage. Therefore, the calculation process considers the entire unloading history.

A number of practical questions were then addressed. It was shown that, (a), as long as the initial convergence does not exceed 50 %, the maximum rock pressure developing upon a practically rigid support that is installed after re-mining a highly deformed tunnel cross section is smaller than the uniaxial compressive strength of the rock irrespective of the overburden (Fig. 5); (b), the maximum re-mining-induced wall convergence occurring in the presence of a light new temporary support can be close to the initial excavation-induced convergence for low stress ratios $\sigma_D/\sigma_0$ (Fig. 6), and particularly in the case of brittle rock behaviour with low residual compressive strength (Fig. 7), while it does not exceed 35 % of the initial excavation-induced convergence for common cases that $\sigma_D/\sigma_0 > 0.15$; and, (c), the construction of an advancing pilot tunnel simply to bring about initial deformations is not beneficial with respect to the excavation of the enlarged tunnel cross section (Figs. 9, 10, 11). These conclusions are based on rigorous, but nevertheless two-dimensional stress analyses.

Finally, it should be noted, although it has not been examined here, that actual re-profiling work is potentially dangerous, especially where the violation of the clearance profile is associated with serious damage to the original support. During re-mining of a highly deformed tunnel segment and installation of the new lining, rock pressure re-distribution occurs in the longitudinal direction, which in turn leads to increasing loads on the already overstressed support. Underpinning of the original support ahead of the re-profiled segment may therefore be necessary.

**Acknowledgments** This paper evolved within the framework of the research project 'Analysis of large deformation problems in tunnelling considering geometric nonlinearities', which is being performed at the ETH Zurich with the financing of the Swiss National Science Foundation (SNF) under Project No. 200021_153433.

## References

Alonso E, Alejano LR, Varas F, Fdez-Manín G, Carranza-Torres C (2003) Ground response curves for rock masses exhibiting strain-softening behaviour. Int J Numer Anal Meth Geomech 27(13):1153–1185

Anagnostou G (2009a) The effect of advance-drainage on the short-term behaviour of squeezing rocks in tunneling. In: Pietruszczak S et al (eds) Proceedings of the International Symposium on Computational Geomechanics (ComGeo I). International Centre for Computational Engineering. Rhodes, Greece, pp 668–679

Anagnostou G (2009b) Pore pressure effects in tunneling through squeezing ground. In: Meschke G et al (eds) Proceedings of the 2nd International Conference on Computational Methods in Tunnelling (EURO:TUN 2009). Aedificatio Publishers, Freiburg, Germany, vol 1, pp 361–368

Bonini M, Barla G (2012) The Saint Martin La Porte access adit (Lyon–Turin Base Tunnel) revisited. Tunn Undergr Sp Technol 30:38–54

Borsetto M, Ribacchi R (1979) Influence of the strain-softening behaviour of rock masses on the stability of a tunnel. In: Wittke W (ed) Proceedings of the 3rd International Conference on Numerical Methods in Geomechanics. Balkema, Rotterdam, vol 2, pp 611–620

Ehrbar H (2008) Gotthard base tunnel, Switzerland: Experiences with different tunnelling methods. In: Proceedings of the 2nd Brazilian Congress of Tunnels and Underground Structures—International Seminar 'South American Tunnelling'. pp 1–14

Hoek E, Guevara R (2009) Overcoming squeezing in the Yacambú-Quibor tunnel, Venezuela. Rock Mech Rock Eng 42(2):389–418

Kovári K (1998) Tunnelling in squeezing rock. Tunnel 98(5):12–31

Kovári K, Staus J (1996) Basic considerations on tunnelling in squeezing ground. Rock Mech Rock Eng 29(4):203–210

Panet M (1976) Analyse de la stabilité d'un tunnel creusé dans un massif rocheux en tenant compte du comportement après la rupture. Rock Mech Rock Eng 8(4):209–223

Panet M (1993) Understanding deformations in tunnels. In: Hudson JA et al (eds) Comprehensive rock engineering: principles, practice and projects, vol 1. Pergamon Press, Oxford, pp 663–690

Rettighieri M, Triclot J, Mathieu E, Barla G, Panet M (2008) Difficulties associated with high convergences during excavation of the Saint Martin La Porte access adit. In: Building underground for the future: Proceedings of the International Congress of Monaco. AFTES, Limonest, France, pp 395–403

Steiner W (1996) Tunnelling in squeezing rocks: case histories. Rock Mech Rock Eng 29(4):211–246

Vogelhuber M, Anagnostou G, Kovári K (2004) Pore water pressure and seepage flow effects in squeezing ground. In: Barla G, Barla M (eds) La caratterizzazione degli ammassi rocciosi nella progettazione geotecnica. Pàtron editore, Bologna, p 495–509

Vrakas A, Anagnostou G (2014) A finite strain closed-form solution for the elastoplastic ground response curve in tunnelling. Int J Numer Anal Methods Geomech 38(11):1131–1148. doi:10.1002/nag.2250

Vrakas A, Anagnostou G (2015) A simple equation for obtaining finite strain solutions from small strain analyses of tunnels with very large convergences. Géotechnique 65(11):936–944. doi:10.1680/geot.15.P.036

Yu HS, Rowe RK (1999) Plasticity solutions for soil behaviour around contracting cavities and tunnels. Int J Numer Anal Methods Geomech 23(12):1245–1279